

Analysis of heuristic function based texture segmentation for enhancing accuracy for ultrasound images compared with unit fuzzy descriptor

Rakesh M¹, Radhika Baskar²

¹Research Scholar, Department of Electronics and Communication Engineering,
Saveetha School of Engineering, Saveetha Institute of Medical and Technical Sciences,
Saveetha University, Chennai, Tamilnadu, India, pin: 602105

²Project Guide, Corresponding Author, Department of Electronics and Communication Engineering,
Saveetha School of Engineering, Saveetha Institute of Medical and Technical Sciences,
Saveetha University, Chennai, Tamilnadu, India, pin: 602105

ABSTRACT

Aim - Pulmonary cell degeneration was known as an important growth factor and the rate of disease tolerance is about 17%. Early detection of tumor in the lungs is a key factor in the degree of endurance. All prominent signs of tumor in the lungs do not appear until the disease has spread to various regions. It requires the appropriate first stage of cellular degeneration in the lungs, to increase the level of endurance. With precise identification, it requires competent exposure and clears the repetition of the duplicate between all the features. **Materials and Methods** - 20 samples taken for this analysis with two groups assigned. Heuristic approach and fuzzy logic were implemented for novel texture segmentation. These groups were analyzed by an independent sample T-test with pretest power of 80%. **Results** - The heuristic approach achieves an accuracy, and sensitivity of 97.25%, 95.22% and fuzzy logic achieves an accuracy, and sensitivity of 95.28% and 88.72%. The obtained significance value is 0.01 for accuracy and 0.03 for sensitivity ($p < 0.05$). **Conclusion** - Heuristic approach achieves significantly better accuracy and sensitivity when compared with fuzzy logic.

Keywords: Image processing, Lung Cancer, Novel Texture Segmentation, Heuristic Approach, Fuzzy Logic, Accuracy, Sensitivity.

INTRODUCTION

Lung cancer is a devastating disease that has killed countless millions of people on a regular basis. The rate of tolerance for a serious illness is about 15%. Evidence suggests that survivors of breast cancer, starvation and colon cancer often did not cause damage to the lung cells. About 60% of patients are male and 33% of girls have cell lung damage. Pulmonary cell degeneration is indicated by uncontrolled cell growth in parts of the lungs. Left unchecked, this progression can spread to the lungs and become metastasis and gradually, to various parts of the body. Because of the large number of tumors that start in the lungs, they are known as important carcinomas that are found in epithelial cells. 80-90% of cell lung damage [1] due to prolonged exposure to tobacco smoke, [2] these cases are often referred to as genetic mixing, [3] radon gas, [3] asbestos, and air pollution including secondhand smoke while non-smokers account for only 10-15% of cellular degeneration in

lung conditions. Symptoms of pulmonary embolism attack the blood. It is a well-known symptom of cellular lung damage. Weight loss will be followed by fatigue and constant tiredness. Cellular degeneration of the lungs can be seen on chest radiographs and tomography (CT filter). By biopsy the conclusion is confirmed [4]. Bronchoscopy or CT-Direct biopsy performs biopsy. Common medications include medical procedures, chemotherapy, and radiotherapy. Treatment and visualization depend on the histological type of fatal growth, stage (spread rate), and the patient's overall well-being, which is measured by the condition of the mortality. Endurance depends on stage, general well-being, and diversity. Typically, 15% of people in India have decided that lung cancer will continue for five years after diagnosis. Globally, pulmonary embolism is the most common cause of malignant growth-related disease in humans, and it is accounted for by more than 1.88 million people every year, since 2008 [5]. The endurance rate of five years of the limited range is probably half. Fatal growth of a limited stage is a disease that does not spread to additional areas such as the lymph hub within the body. Early detection of cellular degeneration in the lungs is a key factor in the endurance rate.

Several scientists have proposed and carried out the finding of lung tumors in the long term in image processing. The paper focuses on the improved segmentation process in Lung Ultrasound images for 78 articles provided by IEEE for review and 102 peer-reviewed articles published by Google scholar. Lung segmentation strategies are divided into four categories [6]–[8]) edge strategies, edge-based strategies, regional-based strategies, and intelligence strategies. The way the lungs appear to be clearly distinct in the regions included in CT scans makes the edge-based techniques more straightforward and effective because of their important requirements that limit the differentiation between lung and tissue ([9]–[11]. In any case, the main damage of the pulmonary embodiment is erroneous because part of the pneumonic parts resembles chest structures. The power of differentiation is derived from the edges under the edge detection channels at various points to detect lung limits from radiographs ([12]–[15]). Each edge point found in the following plan contains a space closure framework for the final stages of aspiration. Depending on how the pixels combine in one place, the localization is made geographically by comparing one pixel with a neighbor by learning the probability that they have the same location. With location-based strategies, the most popular strategy is the site development process [16], [17]. The seeds (small adjustments) are first inserted as a very large growing voxel to remove the lung area to be separated [18]–[20]). Unless local-based strategies are more productive than border-based strategies, they may need to be further developed and re-introduced when undeniable degrees of anomaly are shown in fragmented areas, for example, the chaos from CT knowledge. Canny's techniques include advanced statistics in the field of photographic preparation for segmentation, for example, design acceptance [21], fluffy hypothesis [22], Markov hypothesis [23], and wavelet testing [24], which achieves direct and logical results for lung segmentation in image processing. Previously our team has a rich experience in working on various research projects across multiple disciplines [25]–[35]

In existing approaches, it has drawbacks of lesser accuracy and sensitivity in texture segmentation and lung tumor is a strong contrast in terms of size, thickness and shape, and will be able to participate in a comprehensive, unit development, such as the chest segmentation. The main aim of this work is to implement a texture segmentation using a heuristic approach and comparing its accuracy and sensitivity with a fuzzy logic method.

MATERIALS AND METHODS

In this research, simulation analysis was performed in the Department of Electronics and Communication Engineering, Saveetha School of Engineering. A total of 20 different images were collected for each group. Performances of two groups (heuristic approach & fuzzy descriptor) are evaluated for the same set of images. Sample size was calculated using clinicalc.com, by keeping 0.05 alpha error rate with pretest power 80% . The sample calculation done with previous study [6], [36].

Lung segmentation

The input lung ultrasound cuts which are in JPEG design at first preprocessed in which they are changed over into a grayscale slice. Salt and pepper noise is eliminated utilizing a middle channel which holds the higher esteemed edges in the cuts that are essential for the ROI extraction. Division is done to vary both the left and

right lungs in the ultrasound cut by expulsion of the encompassing areas and undesirable muscles from the slender ultrasound cut (picture). The diverse division strategies are utilized relying upon the segment of the lung that is influenced and furthermore on the sort of illness by which the lung is influenced. So similar segmentation methods can't be utilized for both pleural radiation and pneumothorax. Both the segmentation procedures that are utilized for the division of lungs with pleural emanation and pneumothorax are given to the whole chest ultrasound dataset. The cuts are divided first utilizing the procedure for pleural emission and from there on followed by the division method for pneumothorax [13].

Dataset

Dataset of Lung pictures of 230 are gathered from the Rajiv Gandhi Cancer Institute and Research Center, Chennai, out of which 80 pictures are utilized for testing and 200 pictures are utilized for preparing. Out of 100 pictures which are utilized for testing 45 are cancered Ultrasound pictures and 35 are non-cancered. Also, out of 150 pictures which are utilized for preparing 100 are cancered Ultrasound pictures and 50 are non-cancered. This dataset is developed in MATLAB R2019b.

Texture Features

The texture features are extricated from the gray-level co-occurrence matrix (GLCM). The GLCM constructs the common event of various dark levels a, A between a couple of pixels isolated by a specific distance d and situated at a specific heading θ in a picture space $X \times Y$ (ROI) going from dim level 0 to $Q - 1$ ($Q = 256$) [[37]]. From that point onward, the GLCM component can be characterized as follows:

$$p(a, b) = [(s, t), (u, v)](u - s = x * d, v - t = y * d, A(s, t) = a, A(u, v) = b; \quad (1)$$

Where $(s, t), (u, v)$ are the pixels in ROI, $A(\cdot)$ is the dim level of the pixel, and $\langle \cdot \rangle$ is the quantity of the pixels that meet the search criteria.

Fuzzy descriptor for image segmentation

The main inadequacy of standard FCM calculation is that the target work doesn't consider spatial reliance, thus it manages the picture as equivalent to isolate focus. To diminish the commotion impact during picture division, the proposed technique joins both the nearby spatial setting and the non-neighborhood data into the standard FCM bunch calculation utilizing a novel divergence record instead of the typical distance metric. Along these lines an altered FCM calculation is utilized to portion the picture in our proposed paper. The non-local calculation [38], [39] attempts to exploit the serious level of repetition in a picture. The enrollment esteem chooses the division results and subsequently the participation esteem is assessed by the distance estimation indicated as $k_i d$. Along these lines the methodology alters the distance estimation boundary which is promptly impacted by neighborhood and non-nearby data.

$$distance_{local}^2(a_i, b_j) = \frac{\sum_{a_k \in N_i} (a_k, a_i) distance^2(a_k, b_j)}{\sum_{a_k \in N_i} (a_k, a_i)} \quad (2)$$

$$distance_{non-local}^2(a_i, b_j) = \sum_{a_k \in N_i} (a_k, a_i) distance^2(a_k, b_j) \quad (3)$$

Where $distance_1^2(a_i, b_j)$ represents the distance estimation impacted by neighborhood data, and $\sum_{a_k \in N_i} (a_k, a_i)$ represents the distance estimation affected by non-nearby data, j with the reach from zero to one, is the weighting factor controlling the tradeoff between them.

FCM calculation goes through the accompanying advances,

1. Set the quantity of groups 'c' and the record of fluffiness 'm.' Also introduce the fuzzy descriptor vector 'v' arbitrarily and set >0 to a little esteem,
2. set the local size and the window size incorporates the assessment of bunch focuses and enrollment framework,
3. Assess the changed distance estimation utilizing the condition referenced as $k_i d(x_j, v_i)$,
4. Update the enrollment framework and the distance estimation.

Heuristic approach for novel texture segmentation

In order to image the clinical depiction utilizing K Means bunching calculation, it needs a calculation that can be better for the huge datasets and then find an incentive centroid to liken the achievement. This work depicts a calculation for the division of CT pictures into k diverse that consists of dim, white matter and CSF, and perhaps other surprising tissues. Between scale-esteemed or multi esteemed either can be considered by cut (picture). Each scale-esteemed picture is framed as a get together of regions with relaxed diversifying power with the white Gaussian noise. The lung picture division and the preparing applications, uniquely for the location of disease limits can be utilized by Heuristic approach.

Heuristic approach is considered as idealistic and forcibly investigated model-based way to deal with PC helped clinical picture examination. Heuristic approach image segmentation methodology is given out that is coordinated by précised bound qualities, inverse to standardized first request subordinate profiles, as in the genuine (unique) detailing. A nonlinear classifier is utilized, rather than the linear Mahalanobis distance (interspace), to discover ideal removals/shifts for a region. For every one of the regions or markers that depict the shape, at every goal level considered all through the division improvement strategy, an unequivocal arrangement of ideal highlights is discovered. The determination of highlights is mechanical or programmed, utilizing the preparation pictures and successive elements forward and in reverse choice.

The segmentation of imaging information requires divisioning the picture space into various group clusters with the same intensity picture esteems. The most clinical previews consistently show covering dark scale forces for various tissues. Therefore, fluffy grouping strategies are especially agreeable for the division of clinical depictions. There are a few FCM groupings utilized in the lung division [40]. The fuzzified release of the k-implies calculation is additionally called as FUZZY C-MEANS (FCM) which is a strategy for bunching which permits one piece of information to lie in more than one group. This strategy is by and large utilized in design acknowledgment. The technique that interacts with an ideal c partition by diminishing the weighted inside bunch amount of squared mistake target work is an iterative grouping strategy. Fig. 1 shows the flowchart of texture segmentation using heuristic approach and fuzzy descriptor. It can be classified using a support vector machine.

The proposed Heuristic thresholding strategy to gauge the capacity of the technique in terms of Accuracy, Sensitivity and Specificity measures as,

$$Accuracy = (TP + TN) / (TP + TN + FN + FP) \quad (4)$$

$$Sensitivity = TP / (TP + FN) \quad (5)$$

This work investigated the Rajiv Gandhi Cancer Institute Database and chose from 230 cancer patients. 200 pictures used for testing and preparing picture series are saved in DICOM configuration and recreated to 1320 ROIs in PNG design. To have an equilibrium saving resolution and computational intricacy of the models, the ROI pictures here are trimmed to pixels 512×512 , of which 80 pictures are training information and 20 pictures are testing information. We played out the investigation on the single GPU NVIDIA RTX 2050 utilizing MATLAB R2019b programming language.

RESULTS

Table 1 shows the group statistical analysis of texture segmentation by comparing the accuracy and sensitivity between heuristic approach and fuzzy logic. Fuzzy logic has mean accuracy of 95.28% and sensitivity of 88.72%. Table 2 represents the independent sample T-test for analysing accuracy and sensitivity in texture segmentation. In this statistical analysis, the F-score for levene's test value is 0.85 for accuracy and 0.13 for sensitivity. The obtained significance value was 0.01 for accuracy and 0.03 for sensitivity.

The region overlying the tumor was investigated for chest divider penetration. The shortfall of the pleural relic over the mass was noted, because of the shortfall of circulated air through the lung between the chest divider and the mass. For this situation, the direct sliding of the mass under the parietal pleural surface was utilized to assess invasion is shown in Fig. 2.

In patients with chest divider tumors, the shortfall of the sliding sign hiding the mass was viewed as an indication of lung invasion. For this situation, the pleural antiquity was missing; what's more, unpredictable hyperechogenic lines were available, as an indication of ultrasound reflection at the interface between the mass

and the invaded lung is shown in Fig. 3. Fig. 4 shows the bar graph for representing the comparison of Mean Accuracy and sensitivity of heuristic approach and fuzzy descriptor. The mean accuracy and sensitivity of the heuristic approach is significantly better than the fuzzy descriptor.

DISCUSSION

Novel texture segmentation using heuristic approach achieves significantly better accuracy and sensitivity compared to fuzzy descriptors. The heuristic approach segments the texture with an accuracy of 97.25% and 95.22%. The fuzzy descriptor method segments the texture with an accuracy of 95.28% and sensitivity of 88.72%. By performing the group statistical and independent sample T-test analysis, it is observed that the accuracy and sensitivity of the heuristic approach appears to be better when compared to fuzzy descriptors in texture segmentation.

In the context of clinical picture investigation, the proposed strategies for lung segmentation wipes out the lung limits and isolates the appended right and lungs, which are the two most normal executions in most lung division techniques and require a lot of time [23]. After, to distinguish the sicknesses of lungs knobs utilizing adjusted fuzzy c-means calculation. it achieved an accuracy of 80% due to applied division instruments on a few lung CT pictures. The characterization technique can redesign the speed, strength and precision of finding [22]. It shows an accuracy of 86.5% for pleural emanation and pneumothorax individually. The Heuristic model of lung sickness location for the clinical choice emotionally supportive network dependent on novel combination of the neural organization with heuristics can fill in as clinical choice help ([16], [17]). This work utilized open informational collections with different pneumonic cases and our venture datasets. This synthesis makes us ready to assess how our model functions in discovery of both the normal manifestations just as other pneumonic illnesses. In this work, it had the option to analyze the outcomes and make determinations on how to work on our recommendation toward higher accuracy in anticipated cases yet in addition potentially broaden the utilization of other dis-facilitates. The proposed strategy accomplished better outcomes over our own datasets, which affirms that the proposed model is effective in the event of acknowledgment of pneumonia, sarcoidosis and disease.

The limitation of proposed work is not giving texture segmentation for high pixel images. If saving a JPG or PNG file, the data remains even though the quality of the image has declined. In future, we will attempt to consolidate the segmentation model and lung tissue classification for better CAD of ILD.

CONCLUSION

Novel texture segmentation using heuristic approach segments the texture with an accuracy of 97.25% and 95.22%. The fuzzy descriptor method segments the texture with an accuracy of 95.28% and sensitivity of 88.72%. From statistical analysis, accuracy and sensitivity of heuristic approach achieves significantly better compared to fuzzy logic.

DECLARATION

Conflicts of Interest

No conflict of interest in this manuscript

Author Contributions

Author RA was involved in data collection, data analysis & manuscript writing. Author RB was involved in conceptualization, data validation, and critical review of manuscripts.

Acknowledgment

The authors would like to express their gratitude towards Saveetha School of Engineering, Saveetha Institute of Medical And Technical Sciences (Formerly known as Saveetha University) for successfully carrying out this work.

Funding

We thank the following organizations for providing financial support that enabled us to complete the study.

1. Chipontime Technologies Pvt. Ltd. Bangalore.
2. Saveetha University
3. Saveetha Institute of Medical And Technical Sciences
4. Saveetha School of Engineering

REFERENCES

- [1] D. L. Kasper, A. S. Fauci, S. L. Hauser, D. L. Longo, J. Larry Jameson, and J. Loscalzo, *Harrison's Principles of Internal Medicine 19/E (Vol.1 & Vol.2) (ebook)*. McGraw Hill Professional, 2015.
- [2] D. Liu, "Large Cell Carcinoma and Large Cell Neuroendocrine Carcinoma of the Lung," *Tumors and Cancers*. pp. 65–70, 2017. doi: 10.1201/b22275-13.
- [3] A. J. Alberg and J. M. Samet, "Epidemiology of Lung Cancer," *Murray and Nadel's Textbook of Respiratory Medicine*. pp. 1098–1115, 2010. doi: 10.1016/b978-1-4160-4710-0.00046-8.
- [4] C. Lu *et al.*, "Cancer of the Lung," *Holland-Frei Cancer Medicine*. pp. 1–30, 2017. doi: 10.1002/9781119000822.hfcm085.
- [5] J. Ferlay, H.-R. Shin, F. Bray, D. Forman, C. Mathers, and D. M. Parkin, "Estimates of worldwide burden of cancer in 2008: GLOBOCAN 2008," *International Journal of Cancer*, vol. 127, no. 12. pp. 2893–2917, 2010. doi: 10.1002/ijc.25516.
- [6] A. R. Pulagam, G. B. Kande, V. K. R. Ede, and R. B. Inampudi, "Automated Lung Segmentation from HRCT Scans with Diffuse Parenchymal Lung Diseases," *Journal of Digital Imaging*, vol. 29, no. 4. pp. 507–519, 2016. doi: 10.1007/s10278-016-9875-z.
- [7] A. Mansoor *et al.*, "Segmentation and Image Analysis of Abnormal Lungs at CT: Current Approaches, Challenges, and Future Trends," *RadioGraphics*, vol. 35, no. 4. pp. 1056–1076, 2015. doi: 10.1148/rg.2015140232.
- [8] G. Carneiro *et al.*, *Deep Learning and Data Labeling for Medical Applications: First International Workshop, LABELS 2016, and Second International Workshop, DLMIA 2016, Held in Conjunction with MICCAI 2016, Athens, Greece, October 21, 2016, Proceedings*. Springer, 2016.
- [9] N. Otsu, "A threshold selection method from gray-level histograms," *IEEE Trans. Syst. Man Cybern.*, vol. 9, no. 1, pp. 62–66, Jan. 1979.
- [10] A. R. Amanda and R. Widita, "Comparison of image segmentation of lungs using methods: connected threshold, neighborhood connected, and threshold level set segmentation," *Journal of Physics: Conference Series*, vol. 694. p. 012048, 2016. doi: 10.1088/1742-6596/694/1/012048.
- [11] W. Zhang, X. Zhang, J. Zhao, Y. Qiang, Q. Tian, and X. Tang, "A segmentation method for lung nodule image sequences based on superpixels and density-based spatial clustering of applications with noise," *PLOS ONE*, vol. 12, no. 9. p. e0184290, 2017. doi: 10.1371/journal.pone.0184290.
- [12] E. M. van Rikxoort, B. de Hoop, S. van de Vorst, M. Prokop, and B. van Ginneken, "Automatic Segmentation of Pulmonary Segments From Volumetric Chest CT Scans," *IEEE Transactions on Medical Imaging*, vol. 28, no. 4. pp. 621–630, 2009. doi: 10.1109/tmi.2008.2008968.
- [13] Q. Abbas, "Segmentation of differential structures on computed tomography images for diagnosis lung-

related diseases,” *Biomedical Signal Processing and Control*, vol. 33. pp. 325–334, 2017. doi: 10.1016/j.bspc.2016.12.019.

- [14] A. Gupta, O. Martens, Y. Le Moullec, and T. Saar, “Methods for increased sensitivity and scope in automatic segmentation and detection of lung nodules in CT images,” *2015 IEEE International Symposium on Signal Processing and Information Technology (ISSPIT)*. 2015. doi: 10.1109/isspit.2015.7394363.
- [15] P. Campadelli, E. Casiraghi, and D. Artioli, “A Fully Automated Method for Lung Nodule Detection From Postero-Anterior Chest Radiographs,” *IEEE Transactions on Medical Imaging*, vol. 25, no. 12. pp. 1588–1603, 2006. doi: 10.1109/tmi.2006.884198.
- [16] S. A. Hojjatoleslami and J. Kittler, “Region growing: a new approach,” *IEEE Transactions on Image Processing*, vol. 7, no. 7. pp. 1079–1084, 1998. doi: 10.1109/83.701170.
- [17] M. S. Haleem *et al.*, “A Novel Adaptive Deformable Model for Automated Optic Disc and Cup Segmentation to Aid Glaucoma Diagnosis,” *Journal of Medical Systems*, vol. 42, no. 1. 2018. doi: 10.1007/s10916-017-0859-4.
- [18] J. K. Dash, V. Madhavi, S. Mukhopadhyay, N. Khandelwal, and P. Kumar, “Segmentation of interstitial lung disease patterns in HRCT images,” *Medical Imaging 2015: Computer-Aided Diagnosis*. 2015. doi: 10.1117/12.2079072.
- [19] G. D. Nunzio *et al.*, “Automatic Lung Segmentation in CT Images with Accurate Handling of the Hilar Region,” *Journal of Digital Imaging*, vol. 24, no. 1. pp. 11–27, 2011. doi: 10.1007/s10278-009-9229-1.
- [20] Z. Shi, J. Ma, M. Zhao, Y. Liu, Y. Feng, and M. Zhang, “[ARTICLE WITHDRAWN] Novel Method Using Multiple Strategies for Accurate Lung Segmentation in Computed Tomography Images,” *Journal of Medical Imaging and Health Informatics*, vol. 6, no. 5. pp. 1271–1275, 2016. doi: 10.1166/jmihi.2016.1911.
- [21] J. R. F. Junior, M. Koenigkam-Santos, F. E. G. Cipriano, A. T. Fabro, and P. M. de Azevedo-Marques, “Radiomics-based features for pattern recognition of lung cancer histopathology and metastases,” *Computer Methods and Programs in Biomedicine*, vol. 159. pp. 23–30, 2018. doi: 10.1016/j.cmpb.2018.02.015.
- [22] Q. Mao, S. Zhao, T. Gong, and Q. Zheng, “An Effective Hybrid Windowed Fourier Filtering and Fuzzy C-Mean for Pulmonary Nodule Segmentation,” *Journal of Medical Imaging and Health Informatics*, vol. 8, no. 1. pp. 72–77, 2018. doi: 10.1166/jmihi.2018.2235.
- [23] A. Soliman *et al.*, “Accurate Lungs Segmentation on CT Chest Images by Adaptive Appearance-Guided Shape Modeling,” *IEEE Transactions on Medical Imaging*, vol. 36, no. 1. pp. 263–276, 2017. doi: 10.1109/tmi.2016.2606370.
- [24] O. Talakoub, J. Alirezaie, and P. Babyn, “Lung Segmentation in Pulmonary CT Images using Wavelet Transform,” *2007 IEEE International Conference on Acoustics, Speech and Signal Processing - ICASSP '07*. 2007. doi: 10.1109/icassp.2007.366714.
- [25] D. Ezhilarasan, T. Lakshmi, M. Subha, V. Deepak Nallasamy, and S. Raghunandhakumar, “The ambiguous role of sirtuins in head and neck squamous cell carcinoma,” *Oral Dis.*, Feb. 2021, doi: 10.1111/odi.13798.
- [26] R. Balachandar *et al.*, “Enriched pressmud vermicompost production with green manure plants using *Eudrilus eugeniae*,” *Bioresour. Technol.*, vol. 299, p. 122578, Mar. 2020.
- [27] S. Muthukrishnan, H. Krishnaswamy, S. Thanikodi, D. Sundaresan, and V. Venkatraman, “Support vector machine for modelling and simulation of heat exchangers,” *Therm. Sci.*, vol. 24, no. 1 Part B, pp. 499–503, 2020.
- [28] A. Kavarthapu and K. Gurumoorthy, “Linking chronic periodontitis and oral cancer: A review,” *Oral Oncol.*, p. 105375, Jun. 2021.
- [29] S. C. Sarode, S. Gondivkar, G. S. Sarode, A. Gadbail, and M. Yuwanati, “Hybrid oral potentially malignant disorder: A neglected fact in oral submucous fibrosis,” *Oral Oncol.*, p. 105390, Jun. 2021.
- [30] Hannah R, P. Ramani, WM Tilakaratne, G. Sukumaran, A. Ramasubramanian, and R. P. Krishnan, “Author

response for ‘Critical appraisal of different triggering pathways for the pathobiology of pemphigus vulgaris—A review.’” Wiley, May 07, 2021. doi: 10.1111/odi.13937/v2/response1.

- [31] D. Sekar, D. Nallaswamy, and G. Lakshmanan, “Decoding the functional role of long noncoding RNAs (lncRNAs) in hypertension progression,” *Hypertension research: official journal of the Japanese Society of Hypertension*, vol. 43, no. 7. pp. 724–725, Jul. 2020.
- [32] P. Appavu, V. Ramanan M, J. Jayaraman, and H. Venu, “NOx emission reduction techniques in biodiesel-fuelled CI engine: a review,” *Australian Journal of Mechanical Engineering*, vol. 19, no. 2, pp. 210–220, Mar. 2021.
- [33] S. Menon, H. Agarwal, S. Rajeshkumar, P. Jacqueline Rosy, and V. K. Shanmugam, “Investigating the Antimicrobial Activities of the Biosynthesized Selenium Nanoparticles and Its Statistical Analysis,” *Bionanoscience*, vol. 10, no. 1, pp. 122–135, Mar. 2020.
- [34] R. Gopalakrishnan, V. M. Sounthararajan, A. Mohan, and M. Tholkapiyan, “The strength and durability of fly ash and quarry dust light weight foam concrete,” *Materials Today: Proceedings*, vol. 22, pp. 1117–1124, Jan. 2020.
- [35] V. R. Arun Prakash, J. F. Xavier, G. Ramesh, T. Maridurai, K. S. Kumar, and R. B. S. Raj, “Mechanical, thermal and fatigue behaviour of surface-treated novel Caryota urens fibre–reinforced epoxy composite,” *Biomass Conversion and Biorefinery*, Aug. 2020, doi: 10.1007/s13399-020-00938-0.
- [36] K. Harish Reddy and T. J. Nagalakshmi, “Skin Cancer Detection using Image Processing Technique,” *International Journal of Engineering and Advanced Technology*, vol. 8, no. 6S, pp. 282–285, 2019.
- [37] A. Buades, B. Coll, and J.-M. Morel, “A Non-Local Algorithm for Image Denoising,” *2005 IEEE Computer Society Conference on Computer Vision and Pattern Recognition (CVPR’05)*. doi: 10.1109/cvpr.2005.38.
- [38] R. M. Haralick, K. Shanmugam, and I. ’hak Dinstein, “Textural Features for Image Classification,” *IEEE Trans. Syst. Man Cybern.*, vol. SMC-3, no. 6, pp. 610–621, Nov. 1973.
- [39] A. Buades, B. Coll, and J. M. Morel, “Image Denoising Methods. A New Nonlocal Principle,” *SIAM Review*, vol. 52, no. 1. pp. 113–147, 2010. doi: 10.1137/090773908.
- [40] H. Shamsi and H. Seyedarabi, “A Modified Fuzzy C-Means Clustering with Spatial Information for Image Segmentation,” *International Journal of Computer Theory and Engineering*. pp. 762–766, 2012. doi: 10.7763/ijcte.2012.v4.573.

TABLES AND FIGURES

Table 1. Group statistical analysis of texture segmentation by comparing the accuracy and sensitivity between heuristic approach and fuzzy logic. Heuristic approach has mean accuracy of 95.28% and sensitivity of 88.72%.

Parameter	Group	N	Mean	Std Deviation	Std Error Mean
Accuracy (%)	Heuristic approach	20	97.25	1.03	.375
	Fuzzy Descriptor	20	95.28	1.47	.372
Sensitivity (%)	Heuristic approach	20	95.22	2.25	.621
	Fuzzy Descriptor	20	88.72	2.37	.614

*N-Number of samples

Table 2. The independent sample T-test is analysed for equal variances assumed and equal variances not assumed. In this statistical analysis, the F-score for levene’s test value is 0.85 for accuracy and 0.13 for sensitivity.

		Levene’s test for Equality of Variances		T-test for Equality of Means						
		F	Sig	t	df	Sig. (2-tailed)	Mean difference	Std. Error difference	95% confidence interval of the difference	
									Lower	Upper
Accuracy	Equal Variances assumed	.85	.01	-6.8	48	.000	-3.98	.41	-5.03	-1.92
	Equal Variances not assumed			-6.9	27.9	.000	-3.97	.41	-5.03	-1.92
Sensitivity	Equal Variances assumed	.13	.03	.23	48	.123	.202	.77	-2.49	1.87
	Equal Variances not assumed			.32	27.7	.102	.213	.77	-2.49	1.87

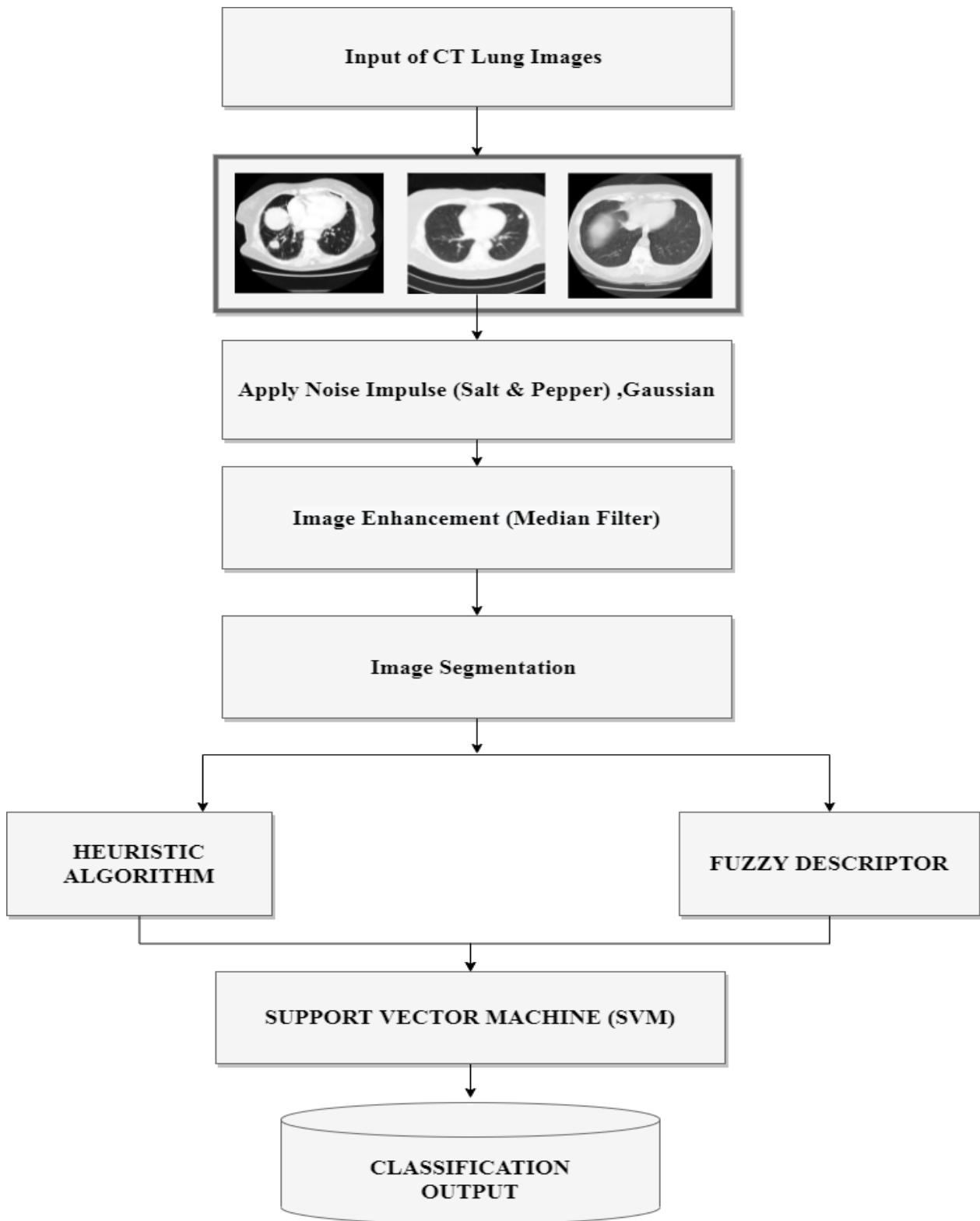


Fig. 1 Flowchart of texture segmentation using heuristic approach and fuzzy descriptor.

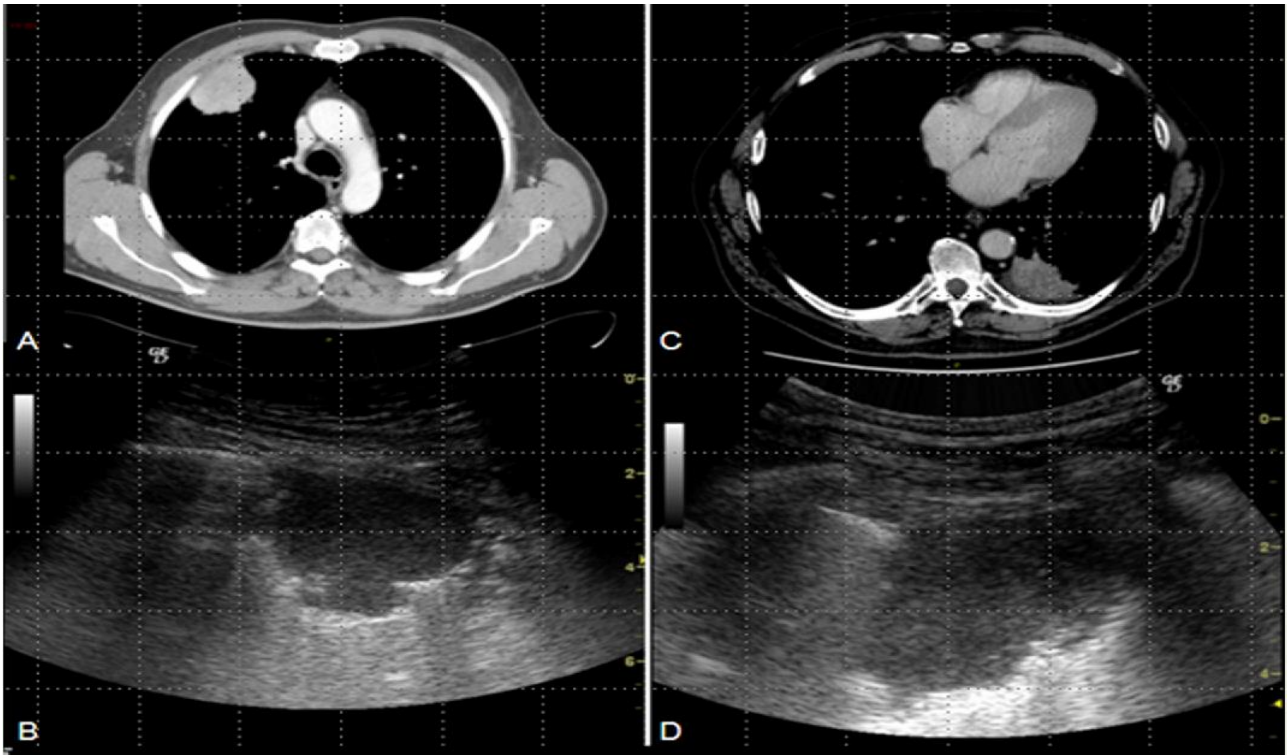


Fig. 2 Peripheral lung tumor image. Fig. 2A and Fig. 2C shows a CT scan with signs of suspect pleural infiltration. Fig. 2B and Fig. 2D shows Ultrasound appearance.

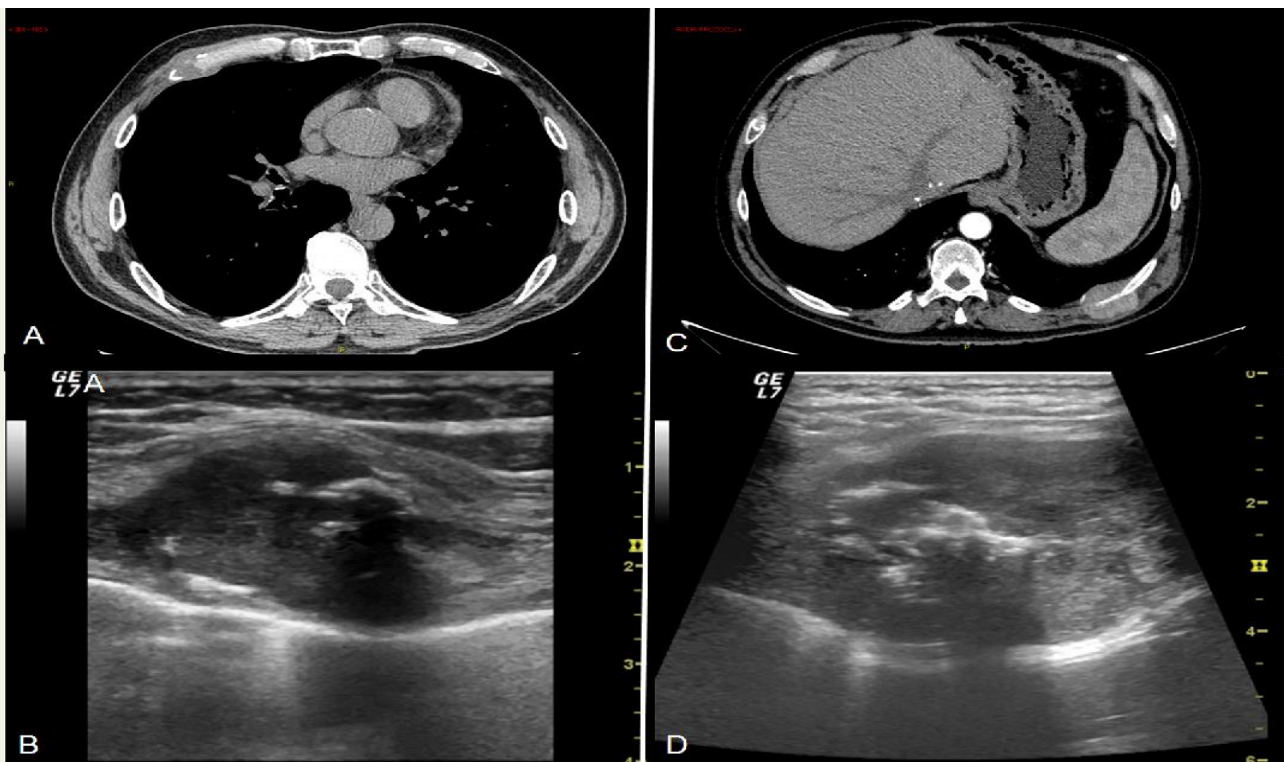


Fig. 3 Lung Wall Cancer. Fig. 3A shows the CT scan of a fifth rib metastasis of colic carcinoma and Fig. 3B shows its Ultrasound image appearance. Fig. 3C shows the CT scan of a tenth rib hepatocarcinoma metastasis. Fig. 3D shows its Ultrasound image appearance.

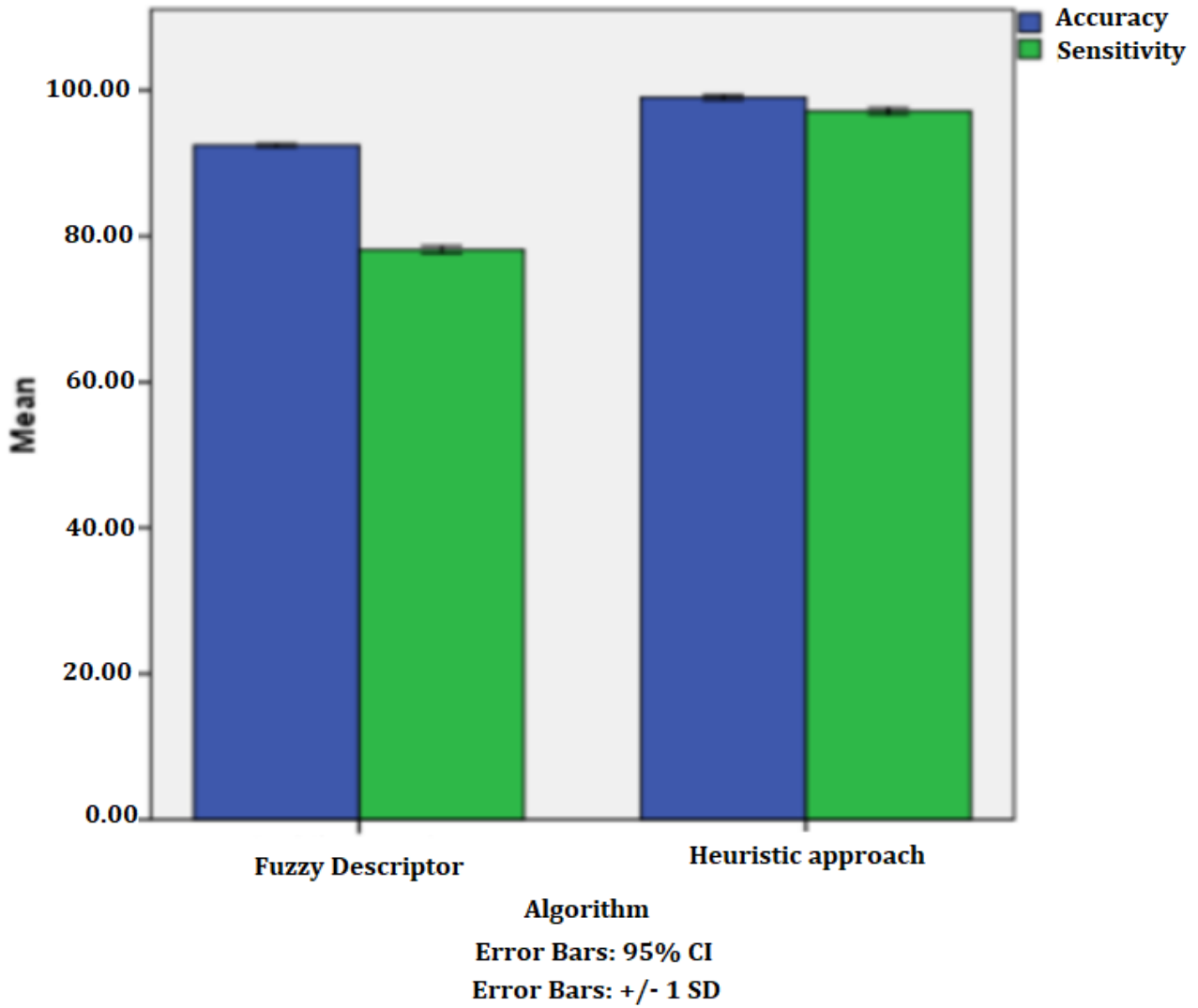


Fig. 4 Bar graph representing the comparison of Mean Accuracy and sensitivity of heuristic approach and fuzzy descriptor. The mean accuracy and sensitivity of the heuristic approach is significantly better than the fuzzy descriptor. X-axis: heuristic approach vs fuzzy descriptor. Y-axis: Mean accuracy and sensitivity of detection 95% CI and ± 1 Standard deviation.